Proceedings of the 19th World Congress
The International Federation of Automatic Control
Cape Town, South Africa. August 24-29, 2014

Preparation of Papers for IFAC Conferences & Symposia: FlipBot: A Lizard Inspired Stunt Robot

C. Fisher* A. Patel**

**University of Cape Town, Cape Town, South Africa (e-mail: fshcal001@myuct.ac.za).*
*** University of Cape Town, Cape Town, South Africa (e-mail:a.patel@uct.ac.za)*

Abstract: Inspired by the acrobatics of the lizard, we present a novel robot platform capable of performing a barrel roll from a ramp. The system is modeled using Euler-Lagrange mechanics, followed by controller design and numerical simulation. A robotic platform is then designed to perform the experiments. Finally, we show that purely by the use of the actuated tail, the robot can rapidly performing a 360 degree roll rotation in under a second.

Keywords: Control, Dynamic modeling, Linearization, Mathematical models, PI controller, Robotics

1. INTRODUCTION

Animal agility still cannot be surpassed by robots. This is understandable considering that the dexterity with which an animal moves is paramount to its survival. These manoeuvres are characterised by a combination of coordination, speed, balance and reflexes. Clearly, for the advancement of future robots we will need to look to Nature for inspiration.

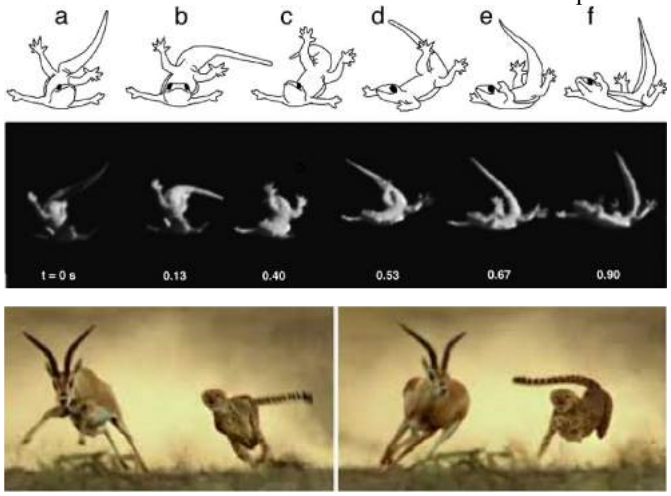

Figure 1: The top image shows a lizard aerially righting its body (Jusufi A. , Active tails enhance arboreal acrobatics in geckos, 2008) and the image below shows a cheetah flicking its tail while making a rapid turn taken from the BBC's "Life of Mammals"

Recent studies have revealed the agility of animals when manoeuvring. Studies have shown that spiders (Chen, Liao, Tsai, & Chi, 2013), cheetahs (Wilson, Lowe, Roskilly, Hudson, Golabek, & McNutt, 2013) and lizards (Libby, et al., 2012) are adapted to manouevre using novel mechanisms. These mechanisms include legs, tails, wings, flexing spine and torso, appendage inertia and pushing off a substrate before an aerial phase (Jusufi, Zeng, Full, & Dudley, 2011).

Tails have many uses in nature as can be seen in Figure 1. Some of these uses include stability, aerial righting, thermoregulation, defence, attack and balance (Briggs, Lee, Haberland, & Kim, 2012).

The cheetah is observed to flick its tail during turning manoeuvres. It has been hypothesized that the tail is providing a reactive torque on the body to prevent it from toppling due to the moment caused by the centrifugal force (Patel & Braae, 2013).

Lizards have been observed to flick their tails to alter their body pitch when jumping from one gradient to another (Chang-Siu, Libby, Tomizuka, & Full, 2011). They have also been observed to use their tails for stability, rapid reorientation and disturbance rejection (Jusufi, Kawano, Libby, & Full, 2010). They achieve this through zero net angular momentum manoeuvres or through direct contact with the surface.

Recently, the robotics community has also seen a resurgence of the use of active tails. The cheetah inspired Dima robot utilises a single degree of freedom tail to achieve turns at much higher speeds than a tail-less platform (Patel & Braae, 2013). The aerial acrobatics of lizards is the source of inspiration for TailBot: a robot which uses a single degree of freedom tail for pitch control (Chang-Siu, Libby, Tomizuka, & Full, 2011). These same authors further demonstrated a two degree of freedom tail capable of 3D aerial righting from a fall (Chang-Siu, Libby, Brown, Full, & Tomizuka, 2013).

There have also been hexapod robots endowed with actuated tails (TAYLRoACH) for turning (Kohut, Pullin, Haldane, Zarrouk, & Fearing, 2013) and the MIT Cheetah robot employed a tail for disturbance rejection (Briggs, Lee, Haberland, & Kim, 2012). A notable result in the research is that tails are more effective for quick manoeuvres than a reaction wheel (Chang-Siu, Libby, Tomizuka, & Full, 2011).

Figure 2: FlipBot the stunt robot.

In the research presented in this paper, we present a lizard inspired stunt robot called FlipBot. This novel platform is capable of performing a 360° barrel roll in mid-air purely by means of actuating its tail as seen in lizards (Jusufi A. , Active tails enhance arboreal acrobatics in geckos, 2008). The paper progresses by first describing the mathematical model of the aerial manoeuvre, followed by a description of the robot design. Following that a controller algorithm design is presented and simulation results are shown. The experimental results are then presented which are followed by a discussion. Finally conclusions are drawn based on these and recommendations made for future avenues of research.

2. Mathematical Modelling

In order to employ the tail for the barrel roll, we first need an understanding of the mechanics of the manoeuvre. Thus, an adequate mathematical model of the system is required.

2.1 The body and Tail System

The system consists of the body and a tail. The body is modelled in 2 dimensions (viewed from behind) and is assumed to be a rectangle with uniformly distributed mass. The wheels of the car are not modelled but are included in the size of the rectangle and also in the total weight of the body. The throttle to the wheels will be cut as the car leaves the ramp and hence the gyroscopic effect of the spinning wheels can be ignored. The system is represented graphically in Figure 3.

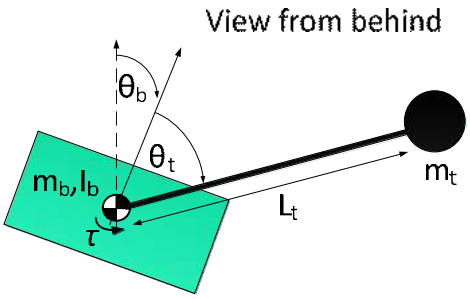

Figure 3: A representation of the system

The tail is modelled as a point mass with no rotational inertia. Following the design procedure of Dima (Patel & Braae, 2013) and TailBot (Chang-Siu, Libby, Tomizuka, & Full, 2011) the mass of the tail was set to 10% of the body mass and the tail length was set to one body length. This resulted in a tail mass of 200 grams and a tail length of 35cm. The tail is a single degree of freedom tail that rotates in the vertical plane when viewed from behind as seen in Figure 3.

2.2 Model of the motor

Two mathematical models of the motor were required for the simulations. The first model related the output torque of the motor to the current speed of the motor and had the following equation (Briggs, Lee, Haberland, & Kim, 2012):

$$\tau_{output} = \tau_{stall} * N * \mu * (1 - \frac{\omega_{motor} * N * \mu}{\omega_{max}}) \quad [1]$$

The next model related the applied terminal voltage to the output torque of the motor. This model had the following equation (Open Source Engineering, 2012):

$$\tau_{output} = \frac{N * K * V_{voltage}}{R} - \frac{N^2 * K^2 * \omega}{R} \quad [2]$$

Where N is the gear ratio, K is the motor constant, R is the terminal resistance, $V_{voltage}$ is the applied voltage to the motor, ω is the relevant velocity, τ is the relevant torque and μ is the motor and gear box efficiency.

2.3 Lagrange Dynamics

The system consists of two general coordinates, θ_b and θ_t. θ_b is the angle between the vertical plane, with respect to the inertial reference frame, the earth, and the vertical of the body. This angle shows how much the body has rolled with respect to the earth. θ_t is the angle between the tail and the vertical of the body. This angle shows how much the tail has rotated due to the torque being applied from the motor.

The fact that the system has linear velocity is neglected as the coordinate system is attached to the body and therefore there is no liner velocity with respect to the coordinate system, only angular velocity.

The linear velocity of the system is observed to determine the time in the air of the system. The car was measured to drive at 5m/s by integrating the accelerometer readings and with a 30 degree ramp this gives 0.7 seconds of air time.

Lagrange Dynamics (Greenwood, 2003) was used to calculate the equations of the system that were simulated in SIMULINK. The equations were as follows:

$$\ddot{\theta}_b = -\frac{L_t * m_t * (\ddot{\theta}_t * L_t - g * \sin(\theta_t + \theta_b))}{(m_t * L_t^2 + I_b)} \quad [3]$$

$$\ddot{\theta}_t = \frac{\tau + L_t * m_t g * \sin(\theta_t + \theta_b))}{(m_t * L_t^2)} - \ddot{\theta}_b \quad [4]$$

These equations define how the system responds over a period of time and are simulated for the length of air time that the system achieves when launched into the air by means of a ramp.

2.4 Assumptions made

- The body is modelled as a rectangle with uniformly distributed mass
- The spinning tyres are not modelled but are included in the size of the rectangle as well as in the mass of the car
- It is assumed that the tail is rotating about the body's centre of mass and that the tail will start in the vertical position
- The moment of inertia of the tail rod is neglected
- The tail is modelled as a point mass with no rotational inertia (Chang-Siu, Libby, Brown, Full, & Tomizuka, 2013)

3. THE ROBOT

3.1 Tail actuator design

In an attempt to eliminate as many design variables as possible the tail length and mass were set to 10% of the body mass and the length of one body length. This leaves three variables that need to be designed for. The first is the motor torque, the second is the motor speed and the third is the gear ratio of the gear box.

Figure 4: SolidWorks model of the tail was designed with an aluminium thread bar with a mild steel mass of 200g.

A simulation of the system equations along with the motor model (equation number 1, 2, 3 and 4) were simulated and the available motors were entered into the simulation. The motor that achieved the highest resulting body angle was selected.

From running simulations the selected motor velocity was 10000 RPM and the stall torque of the motor was rated at 0.0234Nm. The simulation results of the resultant body angle for a period of 0.7 seconds versus the gear ratio of the motor are depicted in Figure 5. As can be seen the optimal gear ratio is 38 but the closest available gear ratio is 50. However, the body still rotates 400 degrees in the required time with no control implemented.

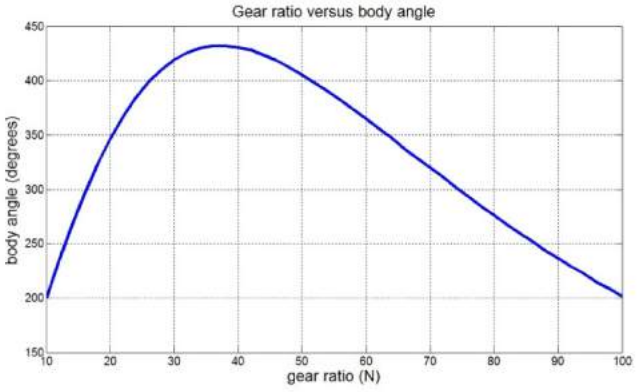

Figure 5: Gear ratio versus body angle. The optimal gear ratio is 38 while the closest available gear ratio is 50.

3.2 Hardware and software

An RC (remote control) car was modified and re-enforced to handle the barrel rolls. A platform to hold all the circuitry was added and a roll cage was included to protect the circuitry. A bracket was added at the back of the car to attach the tail motor. The car weighed a total of 2Kg and the suspension was stiffened to handle the extra load from the tail and the roll cage. Specifications of the car and tail are specified in Table 1 below.

The car communicated with the base station that was connected to a computer that logged the receiving data at 50Hz and an application was written so that commands can be sent to the car.

An STM32 F3 Discovery microprocessor was used as it came with an accelerometer and gyroscope. The code that was used on the robotic platform was written in C and the application was written in C#.

Table 1. Specifications

Tail Motor:	
weight	200g
Torque out	1.17Nm
out RPM	200RPM
ratio	50
voltage	12V
k	0.0055rpm/v
R	1.3Ω
efficiency	80%

The Car	
weight	2kg
size	0.22x0.16x0.35m
I	0.0062 $kg.m^{-2}$
speed	5m/s
The Tail	
weight	200g
length	0.35m
I	0.0245 $kg.m^{-2}$

4. CONTROL SYSTEM DESIGN

4.1 Linearization

In order to apply conventional control theory to the system, to make designing the controller simpler, the nonlinear system was linearized. This was done using Taylor series expansion and the small angle theorem in an attempt to linearize the nonlinear system (Stewart, 2006).

In all cases there was a pole-zero pair in the right hand side and left hand side on the s-plane as well as a double pole at the origin. Depending on the point (θ_b and θ_t) about which the system was linearized, these pole-zero pairs would move on the s axis.

The right half zero caused the body to start rotating in one direction and then after a short period of time it would start rotating in the opposite direction. This non-minimum phase behaviour was an undesirable effect. The pole gets cancelled by the corresponding zero and thus, you can intuitively ignore the effects of these pole-zero pairs.

The linearized system about (0,0) was thus use for control design, and a plant model was given by $g(s) = \frac{-81}{s^2}$. The linear system is a SISO (single input, single output) system with the output being θ_b. The output of the linearized system was compared to the nonlinear system in Figure 6 and it can be seen that they follow the same general shape just the linearized system is 4 times as fast as the nonlinear system and therefore the gains will need to be adjusted when applied to the nonlinear system.

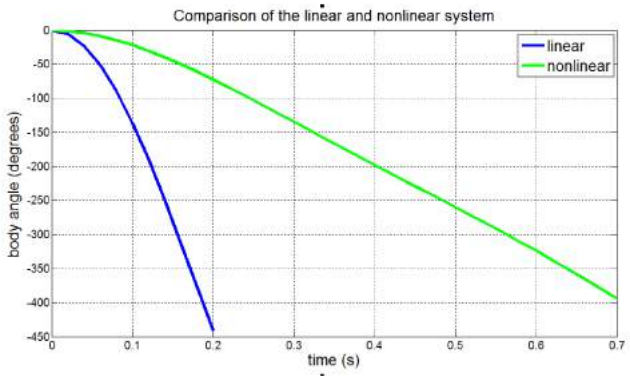

Figure 6: The linear system is shown to be 4 times faster than the nonlinear system. The blue line is the linear system and the green line is the nonlinear system. The graphs are body angle versus time.

4.2 Initial controller design

A PID controller was designed for the linearized system described above. A rise time of 0.5 seconds, a damping factor of 0.707 and an overshoot of 10% were set for the design constraints of the controller. The controller was designed for the continuous system but implemented on the microcontroller as a discrete system with a sampling time of 20ms which resulted in a 50Hz control loop. The step response of the system can be seen in Figure 7.

The effects of a continuous controller operating on a discrete system were ignored due to the fact that the sampling time is small compared to the dynamics of the system. The effect would be a small phase delay in the response of the system. The set point of the controller was a step of 6.28 radians which is equivalent to a full body revolution. The controller had the following form:

$$K(s) = -0.0022086 * \frac{(1 + 0.56s)(1 + 56s)}{s} \qquad [5]$$

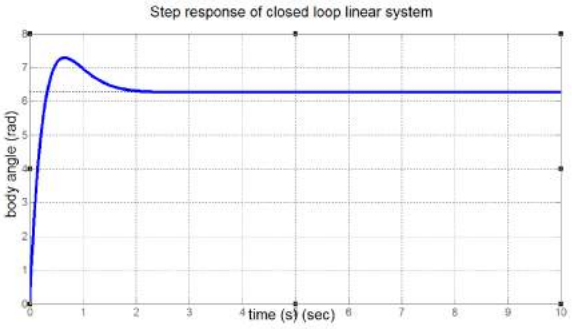

Figure 7: Step response of the closed loop system with a maximum overshoot of 10% and a rise time of 0.5s

The robustness of the designed controller was tested by varying the only unknown in the system, the body moment of inertia, by an increase and then a decrease of 10%. The performance of the controller must be adequate under these conditions in order for it to be implemented on the actual system.

4.3 Revised controller

The designed controller was tested on a simulation of the system equations and a model of the motor (equation number 1, 2, 3 and 4). The controller consisted of an integrator gain, differentiator gain and a proportional gain acting on the error signal. The error signal is calculated by subtracting the body angle from the step set point.

When the controller was tested on the simulated system, the body did not perform a full barrel roll in the required time. This is expected as the linear system is 4 times faster than the nonlinear system. As opposed to performing a gain schedule as there was no tail angle sensor, the gains of the controller were simply modified until the system performed as required. The differentiator gain was small relative to the other gains and was therefore ignored. This resulted in a PI controller with the following form:

$$K(s) = -0.8 * \frac{1 + 2.5s}{s} \qquad [6]$$

The controller enabled the body of the robotic platform to perform a full 360 degree barrel roll in 0.7 seconds. Also, for practical implementation integrator anti wind-up was employed.

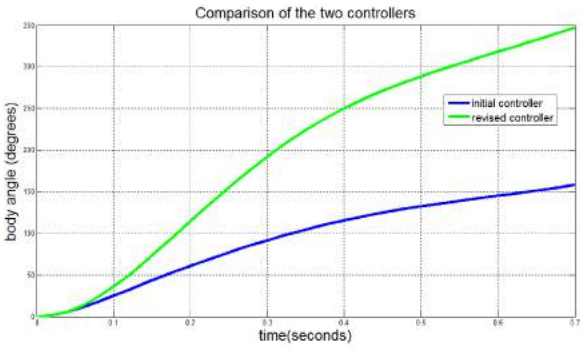

Figure 8: Comparison of the original and revised controllers

As can be seen by the comparison of the two controllers in Figure 8 the original controller does not perform as required but the revised controller successfully controls the full nonlinear system and converges to 360 degrees after 2 seconds with minimal overshoot. This is acceptable because if the system lands at a small angle (under 30 degrees (Chang-Siu, Libby, Brown, Full, & Tomizuka, 2013)) it will flip onto its wheels and complete the barrel roll.

5. EXPERIMENTAL RESULTS

In order to validate the barrel roll manoeuvres on the actual robot platform, the following experimental procedure was performed.

5.1 Test setup

The car drove in a straight line towards the ramp. The ramp was sufficiently far away so that the car reached its maximum speed by the time it reached the ramp. Cameras were set up to record the experiments. The ramp was set at 30 degrees and sufficiently high to achieve the desired air time.

5.2 Un-actuated tail

The first test was to ramp the car without the tail being actuated. This test proves that the car does not have a pitch problem and that the ramp does not aid in rotating the body of the car. The single degree of freedom tail (one control input) can only alter the body roll angle and not the pitch of the body. This can be seen in Figure 9.

Figure 9: un-actuated tail

The next test is with the actuated tail and the results can be compared to this test in order to determine by how much the manoeuvrability of the robotic platform has increased due to the actuated tail.

5.3 Actuated tail

The next set of experiments involved ramping the car and having the tail actuate as the car leaves the ramp. A successful landing can be seen in Figure 10. Data was logged during the test and the applied voltage to the tail motor and the body angle of the system can be seen in Figure 10 and Figure 11. When these graphs are compared to the data from the simulations shown in Figure 11 and Figure 12 it can be seen that they follow the same general shape.

The reason for the sudden increase in gradient of the actual body angle of the system shown in Figure 11 is due to the car hitting the ground at an angle and flipping onto its wheels. If the system was in the air for longer the body angle will follow the simulated curve and will converge to 360 degrees and then land. The impact of the wheels and the ground was not modelled and thus it is different.

Figure 10: Actuated tail. FlipBot performing a complete 360 degree barrel roll

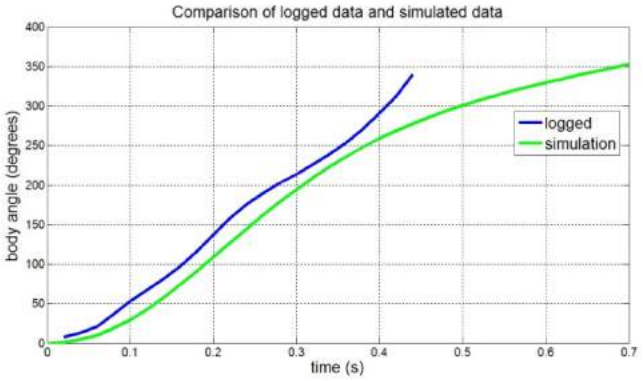

Figure 11: Comparison of the body angle with the simulated results (desired) and the logged data (actual). The graphs follow the same general curve.

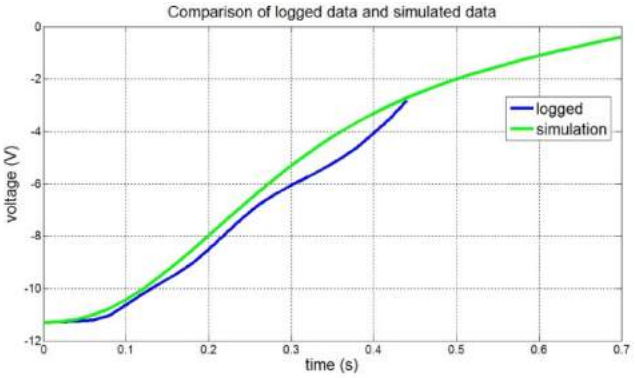

Figure 12: Comparison of the applied voltage to the motor with the simulated results and the logged data. The graphs follow the same general curve.

The initial value of -11volts as shown in Figure 12 is generated by the PI controller due to the fact that the initial error from actual to desired position is 360 degrees.

Comparing this experiment to the previous one it is obvious that the manoeuvrability of the robotic platform has drastically increased due to the active tail.

6. DISCUSSION

From the above results it can be seen that the designed controller for the tail successfully makes the car perform a full 360 degree barrel roll. The accuracy of the model will now be determined. This is achieved in two parts.

The first part is to compare the simulated body angle and control voltage to that of the actual data logged from the car. This is shown in Figure 11 and Figure 12 and it can be seen that they both follow the same general curve.

The second part is to run the simulation from the logged voltage and to compare the body angle of the actual car to that of the simulation, which is being run from the logged voltage being applied to the motor. This comparison is shown in Figure 13 and it can be seen that they follow the same general curve but the simulation only reaches 250 degrees while the car achieved a full 360 degrees.

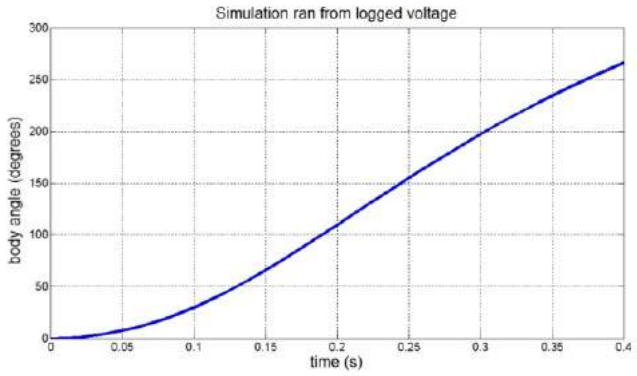

Figure 13: The body angle of the simulation being run from the logged voltage. This can be compared to Figure and it can be seen that they follow the same general curve but the maximum angle achieved is different.

Adjusting the moment of inertia of the car and re-running the experiment until they matched it was shown that the estimated moment of inertia of the car was 50% larger than its actual moment of inertia. The reason why the moment of inertia of the system was changed until the simulation matched the actual was because the moment of inertia of the body is the only unknown in the system.

From analysing the logged data it can be seen that the car only achieves 0.4 seconds in the air. It was calculated that the car will achieve 0.7 seconds. This error is due to the fact that the car slows down when it is travelling up the ramp. The reason why the car still managed to achieve the barrel roll is due to the error in the moment of inertia of the car.

7. CONCLUSIONS

From the above results it can be seen that a simple tail mechanism controlled by a PI controller is capable of making a car achieve a full 360 degree barrel roll in under a second. This demonstrates the power and efficiency of a simple mechanism which has a low mass cost, small space cost and a low computational cost. The model of the system that was determined using Lagrange Dynamics was shown to be accurate despite the error in the moment of inertia of the body. The model was accurate enough to be used to design a controller that will work on the actual system.

To incorporate pitch control into the system a 3 dimensional mathematical model of the system is required, along with a 2 degree of freedom tail. A better estimation of the body's moment of inertia is required.

Partial feedback linearization and optimal control can also be investigated to improve the response of the system.

REFERENCES

Briggs, R., Lee, J., Haberland, M., & Kim, S. (2012). Tails in Biomimetic Design: Analysis, Simulation, and Experiment. *International Conference on Intelligent Robots and Systems (IROS).* Algarve, Portugal: IEEE.

Chang-Siu, E., Libby, T., Brown, M., Full, R. J., & Tomizuka, M. (2013). A nonlinear feedback controller for aerial self-righting by a tailed robot. *International Conference on Robotics and Automation (ICRA).* Karlsruhe, Germany: IEEE.

Chang-Siu, E., Libby, T., Tomizuka, M., & Full, R. J. (2011). A Lizard-Inspired Active Tail Enables Rapid Maneuvers and Dynamic Stabilization in a Terrestrial Robot. *IEEE/RSJ International Conference on Intelligent Robots and Systems (IROS).* San Francisco: IEEE.

Chen, Y., Liao, C., Tsai, F., & Chi, K. (2013). More than a safety line: jump-stabilizing silk of salticids. *Journal of the Royal Society Interface, 10*(87).

Greenwood, D. (2003). *Advanced Dynamics.* Cambridge University Press.

Jusufi, A. (2008, March 18). *Active tails enhance arboreal acrobatics in geckos*. Retrieved October 30, 2013, from PNAS: http://www.pnas.org/content/105/11/4215/F4.expansion.html

Jusufi, A., Kawano, D. T., Libby, T., & Full, R. J. (2010). *Righting and turning in mid-air using appendage inertia: reptile tails, analytical models and bio-inspired robots.* IOP Publishing.

Jusufi, A., Zeng, Y., Full, R. J., & Dudley, R. (2011). Aerial Righting Reflexes in Flightless Animals. *Integrative and Comparitive Biology*, 937–943.

Kohut, N. J., Pullin, A. O., Haldane, D. W., Zarrouk, D., & Fearing, R. S. (2013). Precise Dynamic Turning of a 10 cm Legged Robot on a Low Friction Surface Using a Tail. *International Conference on Robotics and Automation (ICRA).* Karlsruhe: IEEE.

Libby, R., Moore, T., Chang-Siu, E., Li, D., Cohen, D., Jusufi, A., et al. (2012). Tail-assisted pitch control in lizards, robots and dinosaurs. *Nature, 481*, 181-186.

Open Source Engineering. (2012). *Controller For an Inverted Pendulum.* Retrieved November 12, 2013, from Openeering: http://www.openeering.com/sites/default/files/Inverted_Pendulum.pdf

Patel, A., & Braae, M. (2013). Rapid Turning at High-Speed: Inspirations from the Cheetah's Tail. *IEEE/RSJ International Conference on Intelligent Robots and Systems (IROS).* Tokyo: IEEE.

Stewart, J. (2006). *Calculus: Concepts & Contexts 3.*

Wilson, A., Lowe, J., Roskilly, K., Hudson, P., Golabek, K., & McNutt, K. (2013). Locomotion dynamics of hunting in wild cheetahs. *Nature, 498*, 185-189.